Exotic Cluster States in Actinide Nuclei

B. Buck
Department of Physics, Theoretical Physics, University of Oxford, 1 Keble Road, Oxford OX1 3NP, United Kingdom

A. C. Merchant and S. M. Perez*
Department of Physics, University of Oxford, Nuclear Physics Laboratory, Keble Road, Oxford OX1 3RH, United Kingdom
(Received 17 July 1995)

We calculate exotic cluster states for heavy nuclei in the actinide region, using potentials based on an α-core potential which itself reproduces the properties of the low-lying positive parity states of ^{212}Po. We find that by suitably scaling the parameters of the α-core potential so as to reproduce the exotic decay lifetimes, we obtain a good description of the spectra and electromagnetic decay properties of the ground state rotational bands of the actinide nuclei.

PACS numbers: 21.60.Gx, 23.20.–g, 23.70.+j, 27.90.+b

In light nuclei, α-cluster models give a good description of spectra, electromagnetic transitions (and moments), α-emission widths, and α scattering [1–3]. However, α particles are not the only clusters to make their presence felt. There is evidence of ^{3}H and ^{3}He clustering in some nuclei [4], while the observation of resonances in the scattering of light heavy ions (such as ^{12}C, ^{16}O, etc.) [5] suggests the existence of substantially heavier clusters. Indeed, a very successful account of the structure of ^{24}Mg results from a ^{12}C-^{12}C cluster model with mutual excitation of the two components [6]. It has also been suggested that there is significant α clustering in heavy nuclei [7–10], and the phenomenon of exotic decay indicates the presence of heavier clusters in this mass region as well.

Some heavy nuclei in the actinide region are known to decay both by α and by exotic cluster emission. For α decay, we have given a good account of the data using a simple model [11–13] in which the α-core states are characterized by a single value of the global quantum number $G_\alpha = 2n + L \sim 20$, where n is the node number of the radial wave function and L the orbital angular momentum. The α-core potential is given by

$$V(r,R) = V_N(r,R) + V_C(r,R) + \frac{\hbar^2}{2\mu r^2}(L + 1/2)^2, \tag{1}$$

containing nuclear, Coulomb, and Langer-modified centrifugal terms. In addition to a radius R, other parameters such as depth, diffuseness, etc. are generally needed to specify the nuclear potential shape. All such parameters are fixed at globally optimized values, except for the radius R, whose value is tailored for each decay so as to produce an $L = 0$ state at the known decay Q value (corrected for electron shielding [14]). The Coulomb potential $V_C(r,R)$ is generally taken as that arising from a point α cluster and a uniformly charged core of radius R, but for the square well potential we used a surface charge Coulomb force, since this allows analytic evaluation of the half-life for $L = 0$ transitions [11]. From the Bohr-Sommerfeld quantization rule, involving the two innermost classical turning points r_1 and r_2, i.e.,

$$\int_{r_1}^{r_2} dr \sqrt{\frac{2\mu}{\hbar^2}[Q - V(r,R)]} = (2n + 1)\frac{\pi}{2} = (G_\alpha - L + 1)\frac{\pi}{2}, \tag{2}$$

the value of R can be found, and the α-core potential determined. The α-emission width Γ_α is then given by

$$\Gamma_\alpha = \frac{(\hbar^2/4\mu)\exp[-2\int_{r_2}^{r_3} dr\, k(r)]}{\int_{r_1}^{r_2} dr\,[2/K(r)]}, \tag{3}$$

where r_3 is the outermost classical turning point, and the wave numbers are

$$k(r) \text{ or } K(r) = \sqrt{\frac{2\mu}{\hbar^2}|Q - V(r,R)|}. \tag{4}$$

The α-decay half-life is related to the width by $T_{1/2} = \hbar \ln 2/\Gamma_\alpha$. Good fits to the α-decay data can be obtained using various geometries for the α-core potential $V_N(r,R)$, including square-well [11], cosh [12], and the mixed Saxon-Woods form [13]

$$V_N(r,R) = -V_0^{(\alpha)}\left[\frac{x}{1 + \exp[(r - R)/a]} + \frac{1 - x}{\{1 + \exp[(r - R)/3a]\}^3}\right]. \tag{5}$$

Table I shows the parameter values for these geometries which give equivalently good fits to the α-decay data [13].

The data examined above involve ground-state to ground-state favored α transitions, and interest is focused on s-wave α-core states. Once G_α and the potential have been determined, the model gives rise naturally to a band of states with $L = 0, 2, \ldots, G_\alpha$. In analogy with the α-spherical core light nuclei ^{20}Ne and ^{44}Ti, such a band could also describe the low-lying positive parity states of ^{212}Po [15], and for this nucleus the model predictions for

 0031-9007/96/76(3)/380(4)$06.00

Table I. Cluster-core nuclear potential parameter values for various geometries, which produce good fits to α-decay data [13], and the reduction factor f of Eq. (6) required to produce good fits to exotic decay data.

Geometry	G (MeV)	V_0 (fm)	a (fm)	x	f
Square well	24	137	—	—	0.89
Cosh	20	152	0.55	—	0.88
Mixed Saxon-Woods, Eq. (5)	20	238	0.73	0.36	0.92

excitation energies and decays can be compared with experiment [8,13,15]. Good overall fits to decay data *and* the spectrum of ^{212}Po were achieved only by using a potential of the form of Eq. (5) [13].

We have further found that good fits to the exotic-cluster half-lives of actinide nuclei can be obtained from the best-fit potentials for α decay simply by scaling certain parameters. For an exotic cluster of mass A_c, we expect $G_c \sim A_c G_\alpha/4$ and $V_0^{(c)} \sim A_c V_0^{(\alpha)}/4$, with all other parameters fixed at their best-fit values for α decay. The data indicate that we can, in fact, take

$$G_c = A_c G_\alpha/4 \quad \text{and} \quad V_0^{(c)} = f A_c V_0^{(\alpha)}/4\,, \tag{6}$$

where the reduction factor f, obtained by a best fit to the exotic-decay half-lives, is approximately 0.9 for all the geometries considered (see Table I). This scaling is consistent with having more nucleons outside the ^{208}Pb core forming heavier clusters, and with folding model considerations of how the cluster-core potential might be generated. We are developing a more complete treatment of scaling which shows how to construct a universal interaction applicable to any cluster-core system.

An additional $\mathbf{T}\cdot\boldsymbol{\tau}$ isospin-dependent interaction would account for the factor f. This would generate a small repulsive effect for neutron-rich exotic clusters as compared to the self-conjugate α clusters, therefore decreasing the potential depth. The exotic half-lives deduced from the potentials of Table I, using the same techniques as for the α decays, are compared with experiment in Table II. We typically agree to within a factor of 2–3 with the measured half-lives, except for ^{20}O emission. In this case the ratio $(N - Z)/A$ is somewhat larger than the values for the other exotic clusters, so an isospin dependence is again implied. The goodness of fit to the exotic decays is essentially independent of the potential form, as also found for α decay.

It is natural to investigate next the exotic-cluster spectra generated by our potentials. As for α clustering in ^{212}Po [13], only the mixed potential of Eq. (5) gives rise to a simultaneous close correspondence with half-lives and spectra. We have fine-tuned the parameters to optimize these fits, obtaining

$$G_c = 5A_c, \quad V_0^{(c)} = 56.6A_c \text{ MeV}, \quad a = 0.75 \text{ fm}, \quad x = 0.36\,, \tag{7}$$

close to the values deduced directly from the α-decay data [13] shown in Table I. Here we consider only nuclei having exotic decays to the ^{208}Pb ground state, i.e., $^{222}\text{Ra} \rightarrow {}^{208}\text{Pb} + {}^{14}\text{C}$, $^{228}\text{Th} \rightarrow {}^{208}\text{Pb} + {}^{20}\text{O}$, $^{232}\text{U} \rightarrow {}^{208}\text{Pb} + {}^{24}\text{Ne}$, and $^{236}\text{Pu} \rightarrow {}^{208}\text{Pb} + {}^{28}\text{Mg}$. Other cases are easily treated. The exotic half-lives calculated using the parameter values of Eq. (7) are given in Table II, and the corresponding spectra in Figs. 1 and 2 (the fitted R values lie in the range $6.53 \le R \le 6.62$ fm). All the major experimental features of the spectra are reproduced, as, for example, their compression relative to a pure rotational spectrum and the lowering of the 4^+ excitation energies with increasing cluster mass. The excellent agreement already obtained could be improved by fine tuning the parameters for each nucleus.

For a given band the $E2$ strength between states L and $L - 2$ is

$$B(E2; L \rightarrow L-2) = \frac{15}{8\pi}\beta_2^2 \frac{L(L-1)}{(2L+1)(2L-1)} \times |\langle L-2|r^2|L\rangle|^2\,, \tag{8}$$

Table II. Exotic decay half-lives. Comparison of theoretical and experimental half-lives, $T_{1/2}^T$ and $T_{1/2}^E$, respectively, for all known even-even to even-even exotic decays, using values for the parameters of the various potential geometries from Table I and Eq. (7).

Decay	Q (MeV)	Square well $T_{1/2}^T$ (s)	Cosh $T_{1/2}^T$ (s)	Mixed Saxon-Woods Eq. (5) and Table I $T_{1/2}^T$ (s)	Mixed Saxon-Woods Eq. (5) and Eq. (7) $T_{1/2}^T$ (s)	Experiment $T_{1/2}^E$ (s)
$^{222}\text{Ra} \rightarrow {}^{208}\text{Pb} + {}^{14}\text{C}$	33.158	1.28×10^{11}	1.38×10^{11}	1.93×10^{11}	2.21×10^{11}	$(1.01 \pm 0.14) \times 10^{11}$
$^{224}\text{Ra} \rightarrow {}^{210}\text{Pb} + {}^{14}\text{C}$	30.639	5.31×10^{15}	7.36×10^{15}	1.30×10^{16}	1.51×10^{16}	$(8.25 \pm 2.22) \times 10^{15}$
$^{226}\text{Ra} \rightarrow {}^{212}\text{Pb} + {}^{14}\text{C}$	28.316	4.07×10^{20}	7.06×10^{20}	1.55×10^{21}	1.85×10^{21}	$(2.21 \pm 0.96) \times 10^{21}$
$^{228}\text{Th} \rightarrow {}^{208}\text{Pb} + {}^{20}\text{O}$	44.867	3.95×10^{21}	5.64×10^{21}	5.78×10^{21}	6.71×10^{21}	$(5.29 \pm 1.01) \times 10^{20}$
$^{230}\text{Th} \rightarrow {}^{206}\text{Hg} + {}^{24}\text{Ne}$	57.954	3.73×10^{24}	5.16×10^{24}	4.83×10^{24}	5.69×10^{24}	$(4.10 \pm 0.95) \times 10^{24}$
$^{232}\text{U} \rightarrow {}^{208}\text{Pb} + {}^{24}\text{Ne}$	62.492	5.77×10^{20}	5.68×10^{20}	4.75×10^{20}	3.37×10^{20}	$(2.50 \pm 0.30) \times 10^{20}$
$^{234}\text{U} \rightarrow {}^{206}\text{Hg} + {}^{28}\text{Mg}$	74.349	2.30×10^{25}	2.51×10^{25}	2.13×10^{25}	2.53×10^{25}	$(5.50 \pm 1.00) \times 10^{25}$
$^{236}\text{Pu} \rightarrow {}^{208}\text{Pb} + {}^{28}\text{Mg}$	79.896	2.72×10^{21}	1.95×10^{21}	1.42×10^{21}	1.67×10^{21}	4.7×10^{21}
$^{238}\text{Pu} \rightarrow {}^{206}\text{Hg} + {}^{32}\text{Si}$	91.474	6.79×10^{25}	5.64×10^{25}	4.19×10^{25}	2.64×10^{25}	$(1.89 \pm 0.68) \times 10^{25}$

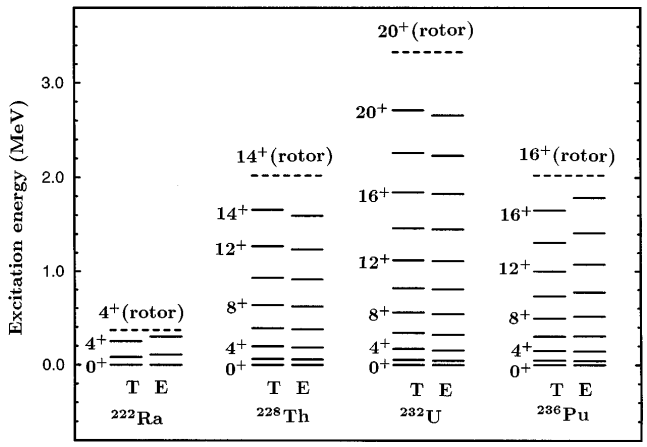

FIG. 1. Exotic cluster spectra, generated by the mixed Saxon-Woods potential of Eq. (5) with parameter values from Eq. (7) (T), compared with experiment (E). The dashed lines show the energy of the highest known spin member of each band expected from a pure rotational model spectrum based on the 2^+-0^+ energy splitting.

where

$$\beta_2 = \frac{Z_1 A_2^2 + Z_2 A_1^2}{(A_1 + A_2)^2}\ , \tag{9}$$

with A_1, Z_1, and A_2, Z_2 being the masses and charges of the ^{208}Pb core and exotic cluster, respectively. Table III shows that the large values of the experimental $B(E2{:}2^+ \rightarrow 0^+)$ values are well reproduced using a moderate effective charge $\epsilon = 0.25e$ throughout. The matrix elements $\langle L - 2|r^2|L\rangle$ do not vary much with L within a given nucleus, nor even from one nucleus to another. This implies that the variation between nuclei with different charges (i.e., different exotic clusters orbiting the ^{208}Pb core) is largely attributable to the differences in the

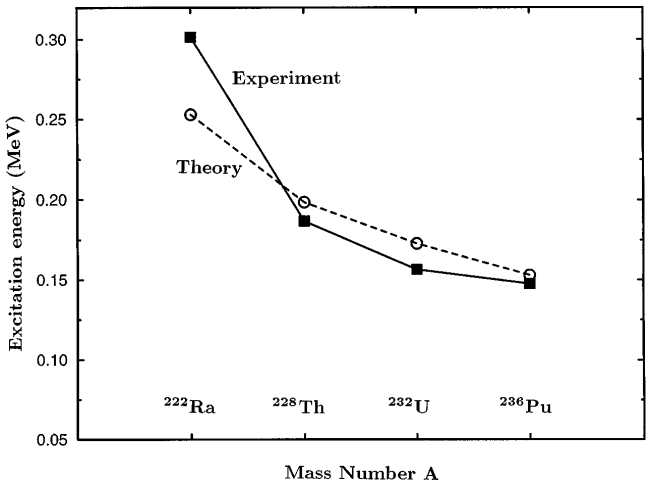

FIG. 2. Excitation energies of 4^+ states, generated by the mixed Saxon-Woods potential of Eq. (5) with parameter values from Eq. (7) (open circles), compared with experiment (solid squares).

Table III. $B(E2\downarrow)$ transition strengths. Comparison of theoretical and experimental $B(E2\downarrow)$ transition strengths, $B(E2\downarrow)^T$ and $B(E2\downarrow)^E$, respectively, using the mixed Saxon-Woods potential of Eq. (5) and with parameters taken from Eq. (7), to generate wave functions. An effective charge of $\epsilon = 0.25e$ is employed throughout. See discussion in text.

Decay	$B(E2\downarrow)^T$ (W.u.)	$B(E2\downarrow)^E$ (W.u.)
^{222}Ra$(2^+ \rightarrow 0^+)$	107	111 ± 9
^{228}Th$(2^+ \rightarrow 0^+)$	170	167 ± 6
^{232}U$(2^+ \rightarrow 0^+)$	250	241 ± 21
^{236}Pu$(2^+ \rightarrow 0^+)$	360	–
^{228}Th$(2^+ \rightarrow 0^+)$	170	167 ± 6
^{228}Th$(4^+ \rightarrow 2^+)$	243	242 ± 9
^{228}Th$(6^+ \rightarrow 4^+)$	267	–
^{228}Th$(8^+ \rightarrow 6^+)$	278	–

factor β_2 of Eq. (9). We then have a natural explanation for the observed discontinuities in $B(E2)$ values as the cluster charge increases, without resorting to the extra parametrization necessary in the collective model. Further, although there is no experimental $B(E2{:}2^+ \rightarrow 0^+)$ value available for ^{236}Pu, we expect the values for all Pu isotopes to be similar, and indeed the measurements for ^{238,240,242,244}Pu of 274 ± 11, 292 ± 10, 298 ± 4, and 300 ± 5 W.u., respectively, are reasonably close to our predicted value for ^{236}Pu. The $B(E2\downarrow)$ variations between different L states of a given nucleus are almost entirely due to the explicit L dependence displayed in Eq. (8). Only ^{228}Th among our chosen ^{208}Pb-core nuclei has a $B(E2\downarrow)$ measurement for any transition other than $2^+ \rightarrow 0^+$, but we predict ratios for $B(E2)$ transition strengths in the ground state bands of all actinide nuclei to be similar. The ratios for $2^+ \rightarrow 0^+{:}4^+ \rightarrow 2^+{:}6^+ \rightarrow 4^+{:}8^+ \rightarrow 6^+$ are predicted to be 1:1.43:1.57:1.65, which compare favorably with the ratios derived for ^{236}U of 1:1.41:1.54:1.59 from the experimental $B(E2\downarrow)$ strengths. This is the only actinide nucleus for which such full results are extant.

Finally, we point out that the model allows a natural explanation of the low-lying excited rotational bands of nuclei in the actinide region. If, for example, the cluster has an isolated first excited 2^+ state, then this will couple with the orbital motion to produce excited $K^\pi = 0^+, 2^+$, and 1^+ rotational bands [16]. Similarly, if the core has a first excited 3^- vibrational state (e.g., as in ^{208}Pb), the composite system will possess the well-known octupole rotational bands. Higher nodal excitations are also possible.

To summarize, we have found, using an exotic-cluster model of the actinides, the following: (1) The rotational ground-state bands, with their level sequences $J^\pi = 0^+, 2^+, \ldots$, are reproduced in a *potential model* without recourse to any special symmetry requirements to remove

the J^π-odd states, employing a potential which also reproduces the ground state exotic decays. The compression of the excitation energies of the high spin members of the bands is obtained, as is the decrease of the excitation energy of a given J^π state with increasing cluster mass. (2) A single moderate value of the effective charge, $\epsilon = 0.25e$ is sufficient to reproduce the pattern of large observed $B(E2)$ strengths in the ground state bands, both for the $L \rightarrow L - 2$ transitions within a single nucleus (which depend mainly on L, since $\langle r^2 \rangle$ remains nearly constant) and also for the variation of $2^+ \rightarrow 0^+$ strengths observed for different nuclei (accounted for mainly by the mass and charge dependence of the different cluster-core identifications).

Although the single core–single cluster description of the various nuclei is very simple, the model has compelling features which will be retained in a more complex cluster-core description.

A. C. M. and S. M. P. thank the U.K. Engineering and Physical Science Research Council (EPSRC) for financial support.

*Permanent address: Department of Physics, University of Cape Town, Private Bag, Rondebosch 7700, South Africa.

[1] K. Wildermuth and Y. C. Tang, in *A Unified Theory of the Nucleus* (Academic Press, New York, 1977), p. 1.

[2] H. Furutani *et al.*, Prog. Theor. Phys. Suppl. **68**, 193 (1980).

[3] B. Buck, in *Proceedings of the 4th International Conference on Clustering Aspects of Nuclear Structure and Nuclear Reactions, Chester, 1984*, edited by J. S. Lilley and M. A. Nagarajan (Reidel, Dordrecht, 1984), p. 71.

[4] A. C. Merchant, J. Phys. G **9**, 1169 (1983); Phys. Lett. **130B**, 241 (1983); J. Phys. G **11**, 527 (1985); Rev. Bras. Fis. **17**, 355 (1986).

[5] K. A. Erb and D. A. Bromley, *Treatise on Heavy Ion Science* (Plenum, New York, 1985), Vol. 3, p. 201.

[6] B. Buck, P. J. B. Hopkins, and A. C. Merchant, Nucl. Phys. **A513**, 75 (1990).

[7] K. Varga, R. G. Lovas, and R. J. Liotta, Phys. Rev. Lett. **69**, 37 (1992); Nucl. Phys. **A550**, 421 (1992).

[8] B. Buck, A. C. Merchant, and S. M. Perez, Phys. Rev. Lett. **72**, 1326 (1994).

[9] F. Hoyler, P. Mohr, and G. Staudt, Phys. Rev. C **50**, 2631 (1994).

[10] S. Ohkubo, Phys. Rev. Lett. **74**, 2176 (1995).

[11] B. Buck, A. C. Merchant, and S. M. Perez, Phys. Rev. Lett. **65**, 2975 (1990).

[12] B. Buck, A. C. Merchant, and S. M. Perez, Phys. Rev. C **45**, 2247 (1992).

[13] B. Buck, J. C. Johnston, A. C. Merchant, and S. M. Perez, Phys. Rev. C **52**, 1840 (1995).

[14] B. Buck, A. C. Merchant, S. M. Perez, and P. Tripe, Phys. Rev. C **47**, 1307 (1993).

[15] B. Buck, A. C. Merchant, and S. M. Perez, Phys. Rev. C **51**, 559 (1995).

[16] D. M. Brink, B. Buck, R. Huby, M. A. Nagarajan, and N. Rowley, J. Phys. G **13**, 629 (1987).